



Microstructural evolution of indirect-extruded ZK60 alloy by adding Ce

Sung Hyuk Park*, Hui Yu, Jun Ho Bae, Chang Dong Yim, Bong Sun You

Light Metal Division, Korea Institute of Materials Science, Changwon 641-831, Republic of Korea

ARTICLE INFO

Article history:

Received 7 June 2012

Received in revised form 3 August 2012

Accepted 5 August 2012

Available online 16 August 2012

Keywords:

Magnesium alloy

Cerium

Extrusion

Dynamic recrystallization

Particle stimulated nucleation

ABSTRACT

The microstructural evolution of an indirect-extruded ZK60 alloy by adding 1 wt.% Ce were investigated. In the extruded condition, the ZK60 alloy shows a bimodal grain structure composed of fine recrystallized grains and coarse unrecrystallized grains, whereas the ZK60-1Ce alloy exhibits a uniformly recrystallized grain structure, resulting from the promotion of dynamic recrystallization during extrusion by particle stimulated nucleation at widely distributed Mg–Zn–Ce particles. The ZK60-1Ce alloy shows a weaker basal texture and higher compressive yield strength than those of the ZK60 alloy due to the decrease in the volume fraction of unrecrystallized grains.

© 2012 Elsevier B.V. All rights reserved.

1. Introduction

It is generally considered that one of the major obstacles to overcome in magnesium extrusions is their low extrusion speed, which is directly related to cost and energy efficiency. Although ZK60 alloy has mechanical properties superior to those of other commercial Mg alloys such as AZ31 and AZ61, the extrusion speed is restricted to 0.5–2.5 m/min, which is far below the speeds attainable with Al alloys [1,2]. This slowness is mainly attributed to an increase in the susceptibility to surface tearing during extrusion, which results from the incipient melting of second-phase particles with low melting temperatures. In this sense, Ce addition in Mg alloys is one method to improve the extrusion speed by forming thermally stable particles containing Ce [3]. In addition, an indirect extrusion process facilitates more rapid extrusion than a conventional direct extrusion process since there is no friction between the billet and the walls of the container and thus no friction heat can occur [4]. However, there has been no investigation of the microstructure of ZK60 alloy with Ce addition produced by the indirect extrusion process. In this study, the microstructure and particle effect of an indirect-extruded ZK60 alloy containing 1 wt.% Ce were investigated.

2. Experimental procedure

The commercial magnesium alloy ZK60 (Mg–5.5 wt.% Zn–0.5 wt.% Zr) alloy was used in the present study as a master alloy. The ZK60 alloy ingots were melted in an electric resistance furnace at 720 °C under an inert atmosphere containing a

mixture of CO₂ and SF₆, then the 1 wt.% Ce (99.9% purity) was added to form the ZK60-1Ce alloy. Melts with/without Ce were held at 720 °C for 30 min, and then poured into a steel mould pre-heated to 200 °C. After casting, the billets were homogenized at 440 °C for 8 h and then water-quenched. Prior to indirect extrusion, billets with 80 mm in diameter and 200 mm long were pre-heated at 250 °C for 1 h in a resistance furnace. Indirect extrusions were conducted at an initial billet temperature of 250 °C, an extrusion ratio of 25, and a ram speed of 1.3 mm/s.

Microstructures were studied using scanning electron microscopy (SEM) and transmission electron microscopy (TEM). The developed texture and grain size of the as-extruded alloys were measured via electron backscatter diffraction (EBSD) installed in a field emission scanning electron microscope (FE-SEM). For the EBSD experiment, automated EBSD scans were performed in the stage control mode with TSL data acquisition software on an area of ~0.04 mm² with a step size of 0.5 μm. Analysis of the EBSD data was accomplished with TSL OIM analysis software and the data with a confidence index of >0.1 were used.

3. Results and discussion

Fig. 1 shows the microstructures of the ZK60 and ZK60-1Ce alloy billets before and after homogenization. Mg–Zn particles formed along grain boundaries in the as-cast ZK60 alloy were mostly dissolved in the α-Mg matrix by homogenization treatment and a few fine particles remained (Fig. 1b). While, a relatively large quantity of Mg–Zn–Ce particles were formed in the as-cast ZK60-1Ce alloy due to the high insolubility of Ce; these Ce containing particles, which had a high melting temperature, were undissolved by the heat treatment and remained at the grain boundaries after homogenization, as shown in Fig. 1d.

Fig. 2a and b provide SEM micrographs of the longitudinal section of the extruded bars. The undissolved particles of the homogenized billets were broken and rearranged along the extrusion direction (ED) during extrusion. The measured volume fractions of the particles were ~0.7% for the ZK60 alloy and ~5.9% for the

* Corresponding author. Tel.: +82 55 280 3516; fax: +82 55 280 3599.

E-mail address: shpark@kims.re.kr (S.H. Park).

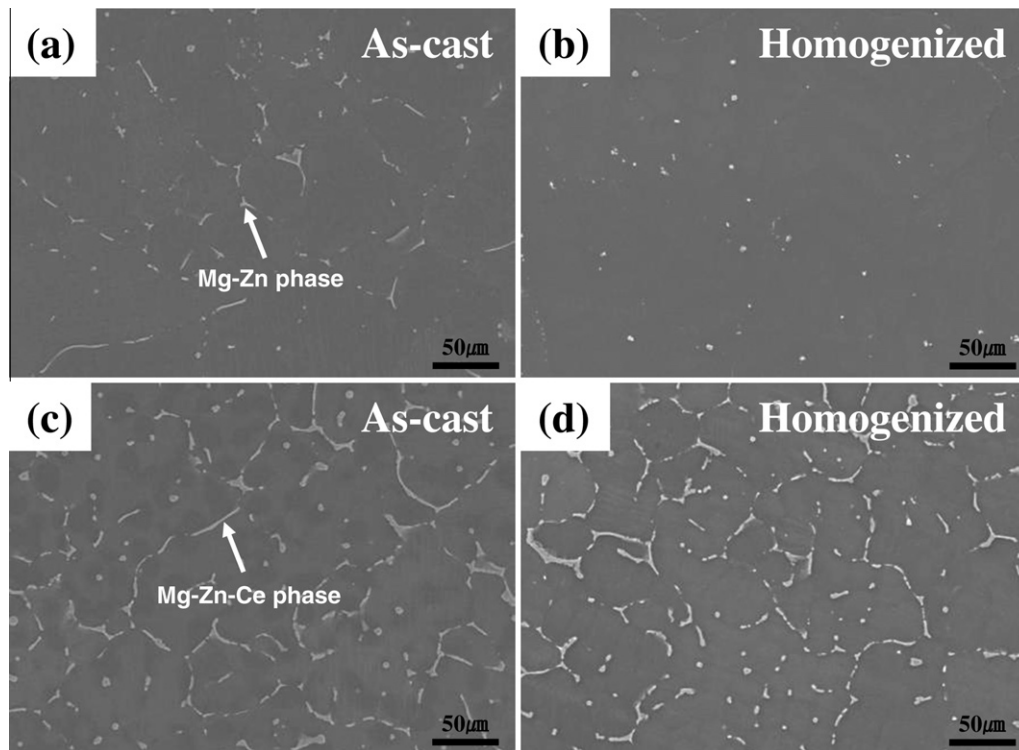


Fig. 1. SEM micrographs of the as-cast and homogenized (a and b) ZK60 and (c and d) ZK60-1Ce alloys.

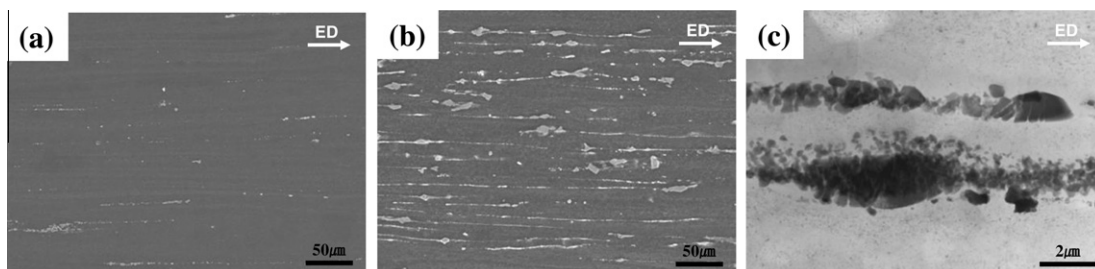


Fig. 2. SEM micrographs showing the shape and distribution of second phase particles of the as-extruded (a) ZK60 and (b) ZK60-1Ce alloys. (c) TEM micrograph showing the detailed morphology of the particles distributed in the as-extruded ZK60-1Ce alloy.

ZK60-1Ce alloy. As can be seen in Fig. 2c, which shows the detailed morphology of the particles distributed in the ZK60-1Ce alloy, the microstructure of the alloy consists of partially broken or unbroken large particles ($>2 \mu\text{m}$ diameter) and totally broken small ones ($\leq 1 \mu\text{m}$ diameter). It is well known that these particles can act as nucleation sites for dynamic recrystallization during hot deformation, i.e. particle stimulated nucleation (PSN) of recrystallization, which affects the grain size and texture of wrought magnesium alloys that have experienced hot deformation processes such as rolling, extrusion and forging [5–7]. It has been reported that the conditions for PSN are such that the particle diameter should be greater than $\sim 1 \mu\text{m}$ [8]. Robson et al. [9] have determined that the effect of large ($>1 \mu\text{m}$ diameter) particles on the recrystallization behavior of magnesium alloys deformed in plane strain compression and shown that the deformation zones surrounding large particles are similar to those seen in other alloys in which PSN occurs. In the AZ41 based alloy, when the size of the isolated coarse particles approaches $2 \mu\text{m}$, some new recrystallized grains occur in the vicinity of the particles by PSN [10].

On the contrary, fine particles smaller than $1 \mu\text{m}$ contribute to the retardation of recrystallization rather than accelerating that

process, by preventing the formation of the lattice curvatures necessary for nucleation via boundary pinning. Even though the individual particles are below the critical size for nucleation ($\sim 1 \mu\text{m}$), a cluster of these particles acts as PSN like one large particle [9,10]. For the ZK60-1Ce alloy, therefore, clusters of fine particles as well as unbroken large particles can also be effective nucleation sites for recrystallization. Furthermore, a high strain of 3.21 imposed through the indirect extrusion process may create more favorable conditions for PSN because the critical particle diameter for PSN decreases with increasing strain.

It was possible to confirm this PSN phenomenon at the Mg–Zn–Ce particles distributed along the ED by comparing the distribution of recrystallized grains and fragmented particles. Fig. 3 shows an inverse pole figure map of the longitudinal section of the as-extruded ZK60-1Ce alloy and its corresponding SEM micrograph. Obviously, it can be seen that the dynamic recrystallization occurs in the region containing the Mg–Zn–Ce particles, as shown in Fig. 3b, while the coarse unrecrystallized grains with blue color, shown in Fig. 3a, correspond to the particle free zone in Fig. 3b. Hence, it is believed that both unbroken large particles and clusters of broken fine particles act as heterogeneous sites for the

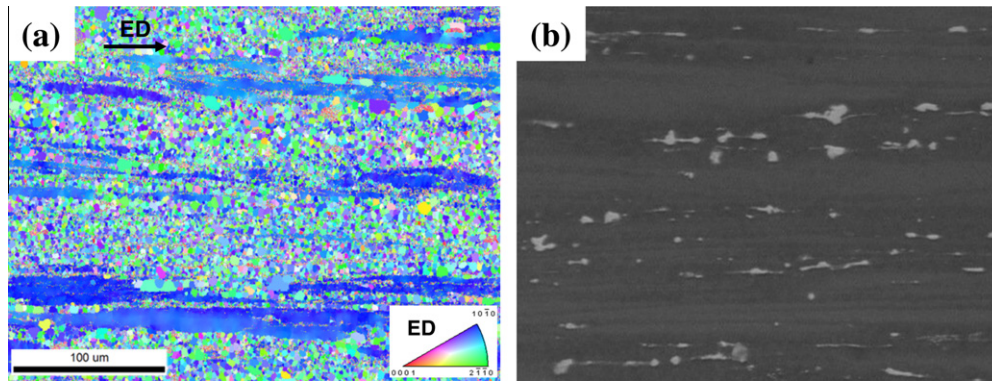


Fig. 3. (a) Inverse pole figure map and (b) corresponding SEM micrograph of as-extruded ZK60-1.0Ce alloy.

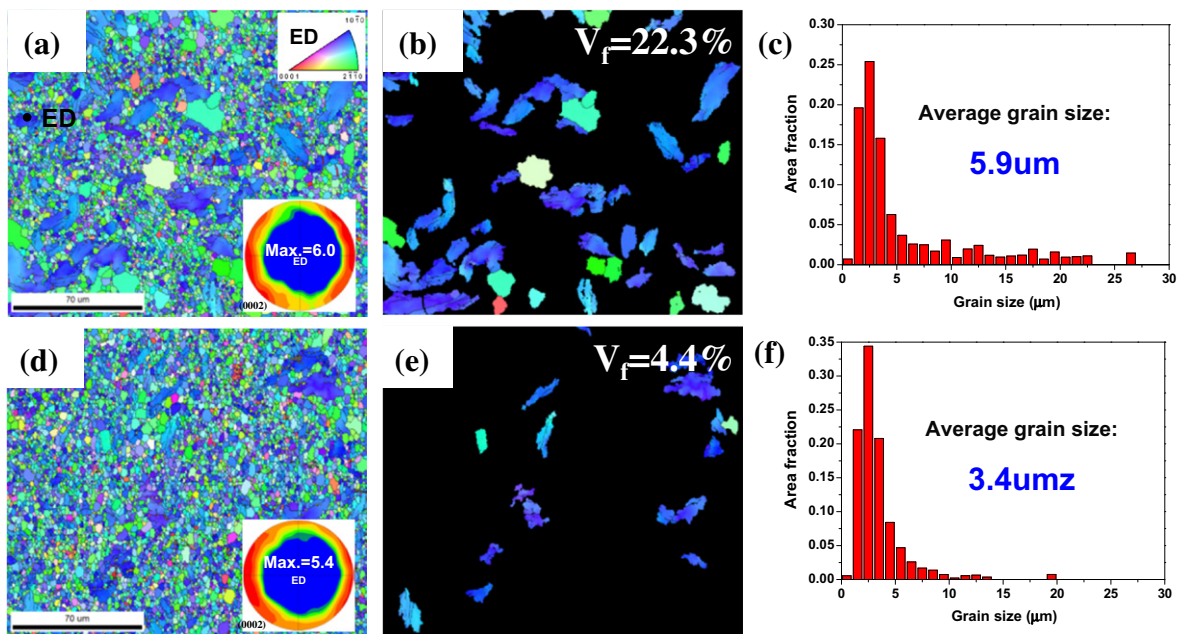


Fig. 4. EBSD measurement results showing the inverse pole figure maps, non-recrystallized area, and grain size distribution of the as-extruded (a–c) ZK60 and (d–f) ZK60-1Ce alloys. The texture plots in (a) and (d) represent the corresponding (0002) pole figures. The volume fraction of the non-recrystallized grains of each material, measured by EBSD, is indicated in (b) and (e).

nucleation of recrystallization by generating local inhomogeneity of the strain energy during the hot extrusion process.

The results of EBSD analysis of the as-extruded ZK60 and ZK-1Ce alloys at a cross-section perpendicular to the extrusion direction are shown in Fig. 4. The ZK60 alloy shows a bimodal grain structure composed of fine recrystallized grains of several microns and coarse unrecrystallized grains larger than 10 μm , while the ZK60-1Ce alloy shows a uniformly recrystallized grain structure. As can be seen in Fig. 4b and e, the volume fraction of the unrecrystallized grains ($\geq 10 \mu\text{m}$) is significantly decreased from 22.3% to 4.4%, resulting from the promotion of dynamic recrystallization during extrusion by widely distributed Mg–Zn–Ce particles with effective size for PSN. Note that the unrecrystallized grains have blue color in the ED inverse pole figure map (Fig. 4b and d); this indicates that these unrecrystallized grains have a strong basal texture in which the prismatic poles tend to orient toward the ED. As shown in the basal pole figures given in Fig. 4a and d, maximum texture intensity decreases from 6.0 to 5.4 with Ce addition. As the texture intensities of the recrystallized area, which are acquired from the EBSD results shown in Fig. 3, have the same value

of 4.6 for the ZK60 and ZK60-1.0Ce alloys, this texture weakening due to Ce addition is attributed to the decreased fraction of unrecrystallized grains with a strong texture. The two alloys both exhibit a typical ring basal texture of extruded Mg alloys (i.e. basal poles aligned perpendicular to the ED); the tilted basal texture due to Ce addition, which is reported by some researchers [11,12], cannot be observed in these alloys. Mishra et al. [11] and McKenzie et al. [13] suggested that the Ce solute changes the grain boundary chemical composition, which in turn affects deformation characteristics during hot deformation and the recrystallization texture of deformed materials. In this study, however, a considerable amount of Ce content added in the ZK60 alloy is thought to be consumed by forming the large Mg–Zn–Ce intermetallic compounds, resulting in a typical extrusion texture after hot deformation, not a tiled basal texture.

The average grain sizes measured from the EBSD data are ~ 5.9 and 3.4 μm , respectively, for the ZK60 and ZK60-1Ce alloys. In the grain size distribution shown in Fig. 4c and f, the size distributions of the recrystallized grains ($< 10 \mu\text{m}$) are nearly identical for two alloys; this means that the Ce addition did not affect the grain size of

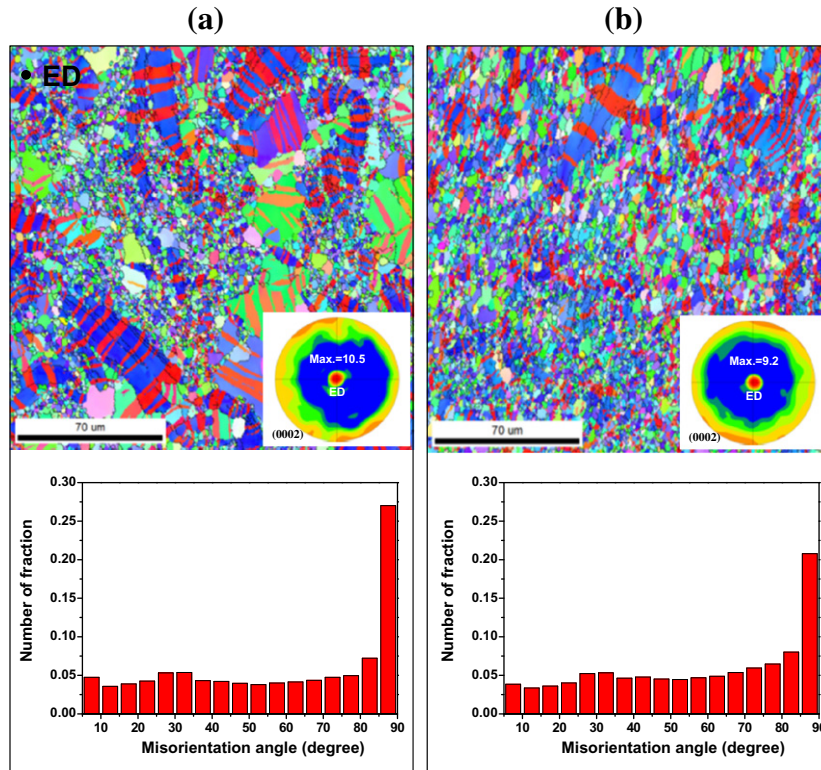


Fig. 5. EBSD measurement results showing the inverse pole figure maps, corresponding (0002) pole figures, and misorientation angle distributions of 2% compressed (a) ZK60 and (b) ZK60-1Ce alloys.

the recrystallized region in the ZK60 alloy. Hence, the decrease in average grain size can be entirely attributed to the decrease in the volume fraction of the large unrecrystallized grains.

To examine the effect of enhanced recrystallization on the twinning behavior, we used cylindrical specimens with height of 12 mm and diameter of 10 mm; the axes of these specimens were oriented parallel to the ED; specimens were compressed to 2% along the ED; then, EBSD analysis was conducted on the cross-sectional areas of the deformed specimens. As compressive load is applied along the ED, the samples are subjected to a loading condition of compression perpendicular to the *c*-axis; this facilitates the {10–12} twinning. As can be seen in Fig. 5, lots of twins were formed by compression, especially in the large unrecrystallized grains. As the effect of grain size on the twinning stress obeys the Hall–Petch relationship and the twinning stress is more sensitive to grain size than the slip stress is [14,15], {10–12} twinning is more easily generated in large unrecrystallized grains than in small recrystallized ones. Moreover, we should note that, compared with recrystallized grains, the unrecrystallized grains, in which the angle between the *a*-axis and the loading axis is close to 30°, are favorably oriented for {10–12} twinning under compression along the ED, because the highest Schmid factor value for {10–12} twinning increases from 0.374 to 0.499 as the angle increases from 0° to 30° [16]. These results indicate that, compared with the ZK60 alloy, the ZK60-1Ce alloy with a small fraction of unrecrystallized grains will twin with difficulty during compression, resulting in a smaller fraction of twinned region and higher compressive yield strength than those characteristics of the ZK60 alloy; the volume fractions of the twinned area and the compressive yield strength are ~13.5% and 242 MPa for the ZK60-1Ce alloy and ~21.4% and 211 MPa for the ZK60 alloy. In the misorientation angle distributions of Fig. 5, the fraction of {10–12} twin boundaries with misorientation angles of 80–90° was also found to be smaller in the ZK60-1Ce alloy than the ZK60 alloy.

4. Conclusions

ZK60 alloy with 1 wt.% Ce addition was subjected to indirect extrusion and the microstructure of extruded alloy was investigated and compared with that of ZK60 alloy. The addition of 1.0% Ce has been shown to significantly promote the dynamic recrystallization during extrusion. The ZK60-1Ce alloy exhibits a more uniform recrystallized grain structure than the ZK60 alloy with a bimodal grain structure composed of fine recrystallized grains and coarse unrecrystallized grains. This promoted recrystallization of the ZK60-1Ce alloy is thought to result from PSN at widely distributed Mg–Zn–Ce particles during extrusion. The Ce addition reduces the volume fraction of the unrecrystallized grains, which have a strong <10–10> texture favorable for {10–12} twinning, and this leads to basal texture weakening and compressive yield strengthening of the extruded alloy.

Acknowledgments

The authors are grateful for the financial support of the Korean Ministry of Knowledge Economy through the “World Premier Materials Program”.

References

- [1] C.J. Bettles, M.A. Gibson, *JOM* 57 (2005) 46–49.
- [2] A.A. Luo, *SAE 2005 Trans.-J. Mater. Manuf.* 114 (2005) 411–421.
- [3] D. Zhang, F. Qi, W. Lan, G. Shi, X. Zhao, *Trans. Nonferrous Met. Soc. China* 21 (2011) 703–710.
- [4] K. Laue, H. Stenger, *Extrusion: Processes, Machinery, Tooling*, American Society for Metals, Ohio, 1981.
- [5] E.A. Ball, P.B. Prangnell, *Scripta Mater.* 31 (1994) 111–116.
- [6] A. Mwembela, E.B. Konopleva, H.J. McQueen, *Scripta Mater.* 37 (1997) 1789–1795.
- [7] A.G. Beer, M.R. Barnett, *Metall. Mater. Trans. A* 38 (2007) 1856–1867.

- [8] F.J. Humphreys, M. Hatherly, *Recrystallization and Related Annealing Phenomena*, 2nd edition., Elsevier, Oxford, 2004. pp. 285–292.
- [9] J.D. Robson, D.T. Henry, B. Davis, *Acta Mater.* 57 (2009) 2739–2747.
- [10] Shouren Wang, Ru Ma, Liying Yang, Yong Wang, Yanjun Wang, *J. Mater. Sci.* 46 (2011) 3060–3065.
- [11] R.K. Mishra, A.K. Gupta, P.R. Rao, A.K. Sachdev, A.M. Kumar, A.A. Luo, *Scripta Mater.* 59 (2008) 562–565.
- [12] A.A. Luo, R.K. Mishra, A.K. Sachdev, *Scripta Mater.* 64 (2011) 410–413.
- [13] L.W.F. Mackenzie, B. Davies, F.J. Humphreys, G.W. Lorimer, *Mater. Sci. Technol.* 23 (2007) 1173.
- [14] M.A. Meyers, O. Vöhringer, V.A. Lubarda, *Acta Mater.* 49 (2001) 4025–4039.
- [15] R.W. Armstrong, P.J. Worthington, *Metallurgical Effects at High Strain Rates*, New York, 1973.
- [16] S.H. Park, S.G. Hong, J.H. Lee, C.S. Lee, *Mater. Sci. Eng. A* 532 (2012) 401–406.